

Evaluation of RISAT-1 FRS-2 Quad Pol Data to be Fully Polarimetric data

Shubham Awasthi¹, Shashi Kumar² and Praveen Kumar Thakur³

^{1,2}Photogrammetry and Remote Sensing Department

³Water Resource Department

^{1,2,3}Indian Institute of Remote Sensing, ISRO
Dehradun, Uttarakhand, India

¹shubham.iirs@gmail.com, ²shashi@iirs.gov.in, ³praveen@iirs.gov.in

KEY WORDS: Synthetic Aperture Radar, Quad polarization, Fully polarimetric data, Phase consistency

ABSTRACT: Synthetic Aperture Radar is a promising technique for monitoring various land cover features. Continuous day and night monitoring of various natural and manmade structures can be done using SAR. The backscatter information from the features can be utilized for microwave imaging. Polarimetric properties of the electromagnetic wave are used to separate different scattering elements available in a single SAR resolution cell. Quad polarized SAR receives the backscatter information which utilizes the four different polarization channels. It adds greater assurance in the results. This Quad-pol data should follow certain conditions to be a fully polarimetric dataset. A fully polarimetric SAR data exhibits the phase coherency across different polarization channels. Hence can be used for various stokes vector based analysis, polarimetric decompositions, phase correlation based studies etc. This paper focuses on the evaluation of the RISAT-1 FRS-2 Quad polarized datasets to be a fully polarimetric SAR datasets. The RISAT-1 FRS-2 and RADARSAT-2 data for the Manali region of date February 2014 were used. In the preprocessing of the datasets radiometric calibration and multi-looking of the datasets was done. The phase coherency between Co-polarized channels i.e. relative phase between HH and VV was evaluated. The degree of polarization and the stokes parameter conditions were also analyzed. The RISAT-1 FRS-2 phase distribution curve was compared with the same obtained from Radarsat-2 fully polarimetric data. The Radarsat-2 showed characteristic relative phase curves matching to the theoretical PDF (Power Distribution curve). RISAT-1 FRS-2 was having incoherency in between co-polarized channels HH and VV. The RISAT-1 FRS-2 was found inconsistent for considering it as a fully polarimetric data. This made this data not suitable for the generation of relative phase (HH-VV), generation of coherency matrix, calculating stokes parameters and polarimetric decomposition.

1. INTRODUCTION

Microwave remote sensing using SAR (Synthetic Aperture Radar data) has the potential of monitoring various land cover targets as well as retrieving the target parameters because of its unique sensitivity to the geometrical, structural and dielectric properties of the target. From the past few years with the development of quad-pol sensors like Radarsat-2, TerraSAR-X and ALOS PALSAR-2 preference to the fully Polarimetric SAR data is given to extract better information. This data provides the comprehensive polarimetric information which allows both model based decompositions and Eigen value based decomposition. These datasets using Polarimetric SAR (PolSAR) systems can be used to separate out the different scattering mechanisms-single bounce, double bounce and volume scattering mechanisms available in single SAR resolution cell. It is done by analyzing the polarization state of various polarimetric channels received after being backscattered from various man-made and natural targets (Lee & Pottier, 2009). It is useful in order to extract the qualitative and quantitative information of various targets like vegetation, land, ocean and snow. The quad-pol SAR sensor transmits the microwaves in the Horizontal (H) and vertical (V) polarizations simultaneously and receives in four polarization channels HH, HV, VH and VV. For the correct information retrieval from the backscatter microwave, the phase coherency between the polarization channels of the quad-pol data should be there. It should also follow the monostatic condition and should have high degree of polarizations. The degree of polarization is the ratio of polarized power to the total power received from the microwave sensor. This paper focusses on the evaluating the RISAT-1 FRS-2 quad-pol data for pertaining to be the fully polarimetric datasets. Various conditions for this data to be fully polarimetric is analyzed. Phase consistency, the monostatic condition and degree of polarization is also evaluated for this study. The comparative analysis with the Radarsat-2 dataset has also been done.

2. STUDY AREA AND DATASETS USED

2.1 Study Area

The Beas River Basin up to Manali town with area of 350.21 km² has been selected for this study, in the state of Himachal Pradesh situated in Northern India. The area is at an altitude of 4350 m above mean sea level, 51km north of Manali. The terrain is relatively undulating and is a part of North-Western Himalayas.

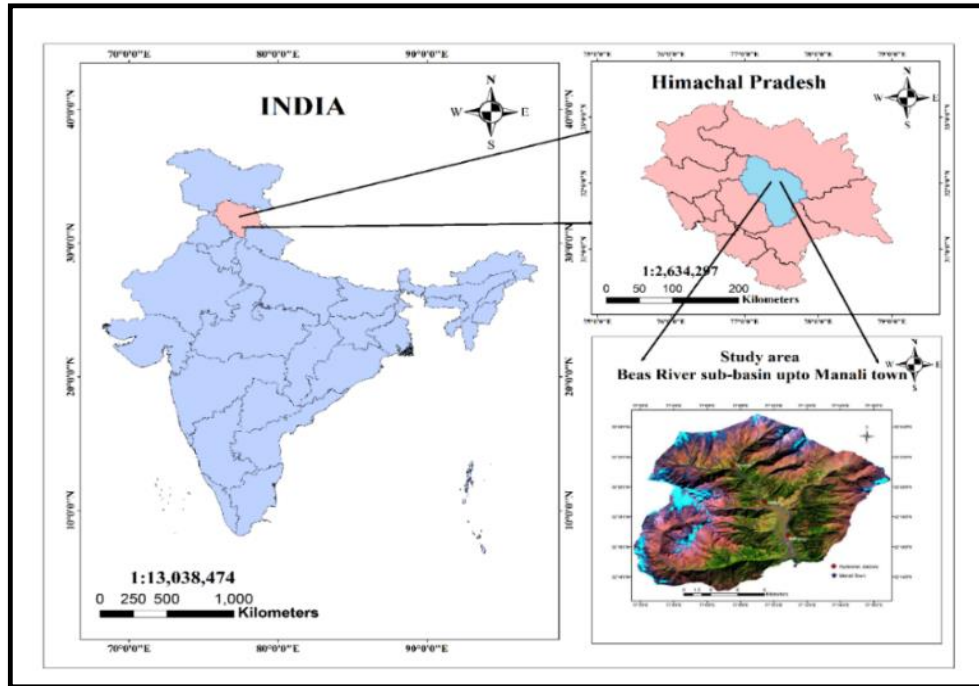


Figure 1- Study Area

2.2 Datasets Used

The two datasets RISAT-1 in FRS-2 quad pol mode and Radarsat-2 datasets were used in this study. The comparative analysis between the RISAT-1 FRS-2 and Radarsat-2 was done as both the datasets operate in the C band and has the

Description	Dataset-1	Dataset-2
Satellite	RISAT-1 FRS-2	RADARSAT-2
Date of acquisition	23-2-2014	25-2-2014
Time of acquisition	12:55:32 UTC	10:19:39 UTC
Image Id	1428550131	PDS_03512070
Polarizations	HH, VV, HV, VH	HH, VV, HV, VH
Centre frequency	5.35 GHz	5.405 GHz
Acquisition mode	FRS-2	Fine Quad Polarization
Incidence angle	49.044°	39.19°
Centre lat/long	29°14'05" N, 79°21'07" E	29°14'05" N, 79°21'05" E

Table 1-SAR data Specification

3. METHEDODOLOGY

3.1 Methodology flow diagram: -

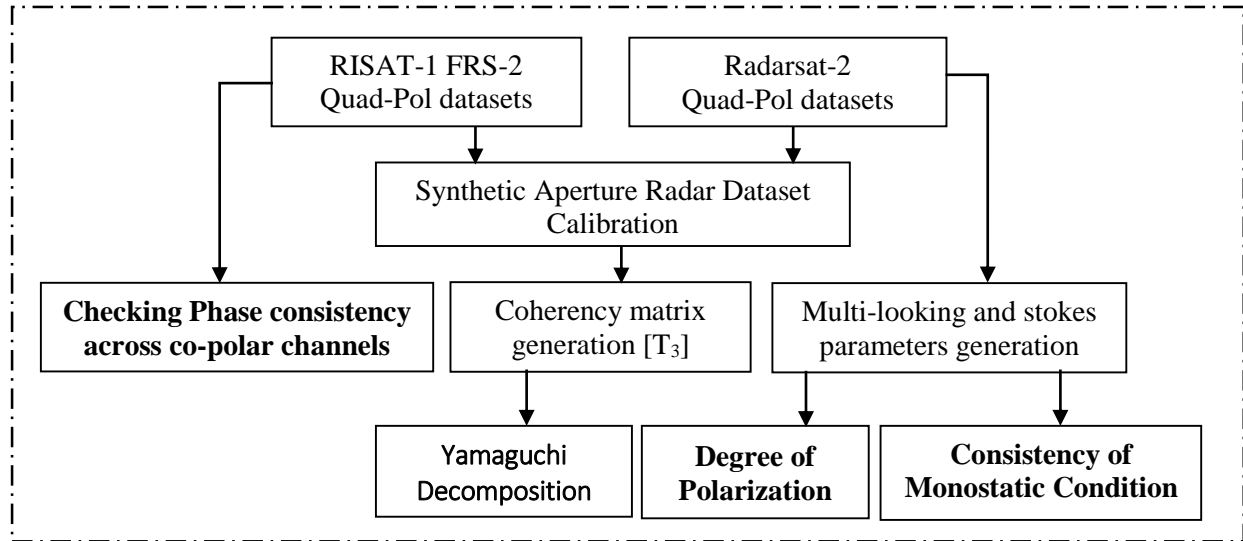


Figure 2-Methodology flow diagram

3.2 RISAT-1 FRS-2 and RADARSAT-2 data processing

3.2.1 Calibration of the data

Calibration is the process of quantitatively defining the signal responses to a known controlled signal inputs. After the radiometric calibration of the SAR data, it is possible to compare the values obtained by different SAR sensors and also with the ground based observations. For SAR images the Digital Number (DN) value is directly related to the received voltage in the SAR sensor. Also, the image intensity too is proportional to the received power. The process to retrieve backscatter coefficient from the observed SAR image intensity is known as the radiometric calibration (Mishra & Patel, 2015; Rao, Meadows, & Kumar, 2016). Calibration has been performed over the given dataset according to the relation given below:

$$\sigma = (DN)_p \times \sqrt{\frac{\sin(ip)}{\sin(ic)}} \times \frac{1}{\sqrt{10(k/10)}} \quad (1)$$

3.2.2 Scattering Matrix Generation

For the quad pol datasets, the EM waves are transmitted in the horizontal and the vertical polarizations. The change in the polarization plane is experienced by the EM wave after being backscattered from the targets. At the receiver the received electromagnetic waves can be represented in the form of a 2x2 scattering matrix:-

$$[S] = \begin{bmatrix} S_{HH} & S_{HV} \\ S_{VH} & S_{VV} \end{bmatrix} \quad (2)$$

The complex backscatter information of the target in all the four polarizations is represented by this matrix. This complex backscatter contains both phase and the magnitude information with it.

3.2.3 Coherency matrix generation

The coherency matrix gives the second order scattering mechanism information. This matrix is obtained from the Hermitian product of the Pauli basis and describes the local variations in the scattering. The vectorized form of the scattering matrix in Pauli format is given as:-

$$k_p = \frac{1}{\sqrt{2}} \begin{bmatrix} S_{HH} + S_{VV} \\ S_{HH} - S_{VV} \\ 2S_{HV} \end{bmatrix} \quad (3)$$

The coherency matrix so obtained is given by:-

$$\langle [T] \rangle = \langle k_p k_p^\dagger \rangle \quad (4)$$

where \dagger represents complex conjugate and represents the average over the whole data. The coherency matrix obtained using (3) is given as

$$\langle [T] \rangle = \begin{bmatrix} \langle |S_{HH} + S_{VV}|^2 \rangle & \langle (S_{HH} + S_{VV})(S_{HH} - S_{VV})^* \rangle & 2\langle (S_{HH} + S_{VV})S_{HV}^* \rangle \\ \langle (S_{HH} - S_{VV})(S_{HH} + S_{VV})^* \rangle & \langle |S_{HH} - S_{VV}|^2 \rangle & \langle (S_{HH} - S_{VV})S_{HV}^* \rangle \\ 2\langle S_{HV}(S_{HH} + S_{VV})^* \rangle & 2\langle S_{HV}(S_{HH} - S_{VV})^* \rangle & 4\langle |S_{HV}|^2 \rangle \end{bmatrix} \quad (5)$$

Elements T_{11} , T_{22} and T_{33} are sensitive to surface, double bounce and volume scattering from a single SAR resolution cell. The sum of the diagonal elements represents the total backscattered power of wave. Also the Eigen values of both the covariance matrix and coherency matrix are same.

3.2.4 Yamaguchi Decomposition

Yamaguchi decomposition is a model based technique which represents the coherency matrix into sum of four scattering mechanisms- Surface scattering, Double bounce scattering Volume scattering and Helix scattering (Yamaguchi, Yajima, & Yamada, 2006). The total power is distributed between the various scattering mechanisms by applying modelling approaches.

$$\langle [T] \rangle^{HV} = f_s [T]_{surface}^{hv} + f_d [T]_{double}^{hv} + f_v [T]_{vol}^{hv} + f_c \langle [T] \rangle_{helix}^{hv} \quad (6)$$

Here Coherency matrix T_3 as the sum of powers in the surface scattering, double, volume and Helix scattering mechanisms in eq-6.

$$[T_3] = f_s \begin{bmatrix} 1 & \beta^* & 0 \\ \beta & |\beta|^2 & 0 \\ 0 & 0 & 0 \end{bmatrix} + f_d \begin{bmatrix} |\alpha|^2 & \alpha & 0 \\ \alpha^* & 1 & 0 \\ 0 & 0 & 0 \end{bmatrix} + \frac{f_v}{2} \begin{bmatrix} 2 & 0 & 0 \\ 0 & 1 & 0 \\ 0 & 0 & 1 \end{bmatrix} + \frac{f_c}{2} \begin{bmatrix} 0 & 0 & 0 \\ 0 & 1 & \pm j \\ 0 & \pm j & 1 \end{bmatrix} \quad (7)$$

Here β and α the surface bounce and the double bounce parameters, derived using X-Bragg's coefficient and Fresnel reflection coefficient respectively. f_s , f_d , f_v and f_c are the expansion coefficients. For more detailed study of this decomposition model (Yamaguchi, Moriyama, Ishido, & Yamada, 2005) can be referred.

3.2.5 Degree of polarization (m)

Degree of polarization quantifies the amount of wave polarized to that of it that is not polarized i.e. it is the ratio of the power of polarized wave to the total power of the electromagnetic wave. Its value lies between 0 and 1. It is an indicator of polarized and diffused scattering. If m is equal to 1, it implies that the wave is fully polarized and is equal to zero for a partially polarized wave.

$$m = \frac{\sqrt{s_1^2 + s_2^2 + s_3^2}}{s_0} \quad (8)$$

The degree of polarization varies 0 to 1. For fully polarimetric data the value of the Degree of polarization should be 1.

3.2.6 Co-polarization phase difference

A fully polarimetric data has phase coherency across the co-polarized channels HH and VV. The Polarimetric Co-polar coherence (HH and VV) correlation between the co-polarized phase channels HH and VV in the multi-Polarimetric radar. The normalized complex correlation coefficient is calculated as the average of the product between the complex amplitude of the HH channel and the conjugate of the complex amplitude of the VV channel. The normalization of the product is done by dividing the product by the square root of the product of the powers in the HH and VV channels. If the value of correlation coefficient is one, then both polarization channels are linearly related. If the value of the complex correlation coefficient is less than one, it indicates the phase delay between the polarization channels HH and VV which ultimately means they are not directly related. It also indicates that noise is present on one of the two channels.

$$\tilde{\gamma}_c = \gamma_c \cdot e^{i\phi_c} = \frac{\langle S_{VV} S_{HH}^* \rangle}{\sqrt{\langle |S_{VV}|^2 \rangle \cdot \langle |S_{HH}|^2 \rangle}} \quad (9)$$

CPD can be defined as the ensemble average of the co-polarized phase difference between HH and VV polarization channels in a multi-polarized or polarimetric radar (Leinss, Parrella, & Hajnsek, 2014). It is the phase angle of the co-pol correlation coefficient (Rodionova, 2009). The co-polar phase difference can be used to classify the image. The single bounce has the co-pol phase difference of 180° while an ideal double bounce (or even-bounce) scatterer will have a co-polar difference as 0°. For the volume scatters the value of CPD lies between -180° to 180°. The cross phases does not show any such correlations between the channels hence cross polar phase difference is insignificant. It is uniform for the most of the features but co-polar phase difference shows Gaussian Power distribution function.

$$\phi_c = \phi_{HH} - \phi_{VV} = \frac{\langle \text{Im}(S_{VV} S_{HH}^*) \rangle}{\langle \text{Re}(S_{VV} S_{HH}^*) \rangle} \quad (10)$$

ϕ_c is the co-polarimetric phase difference (CPD) and the S_{HH} and S_{VV} are the Horizontal and vertical co-polar channels in Single complex look data.

4 RESULTS

4.1 Checking Phase coherency between HH and VV Channels and Yamaguchi Decomposition

The fully polarimetric datasets have the property of phase coherency across co-polar channels HH and VV. Hence further stokes parameter based analysis and polarimetric decomposition can be possible. Here the assessment of the co-polar phase coherency is done by calculating the relative phase across the polarization channels and the Yamaguchi decomposition is applied for both the datasets.

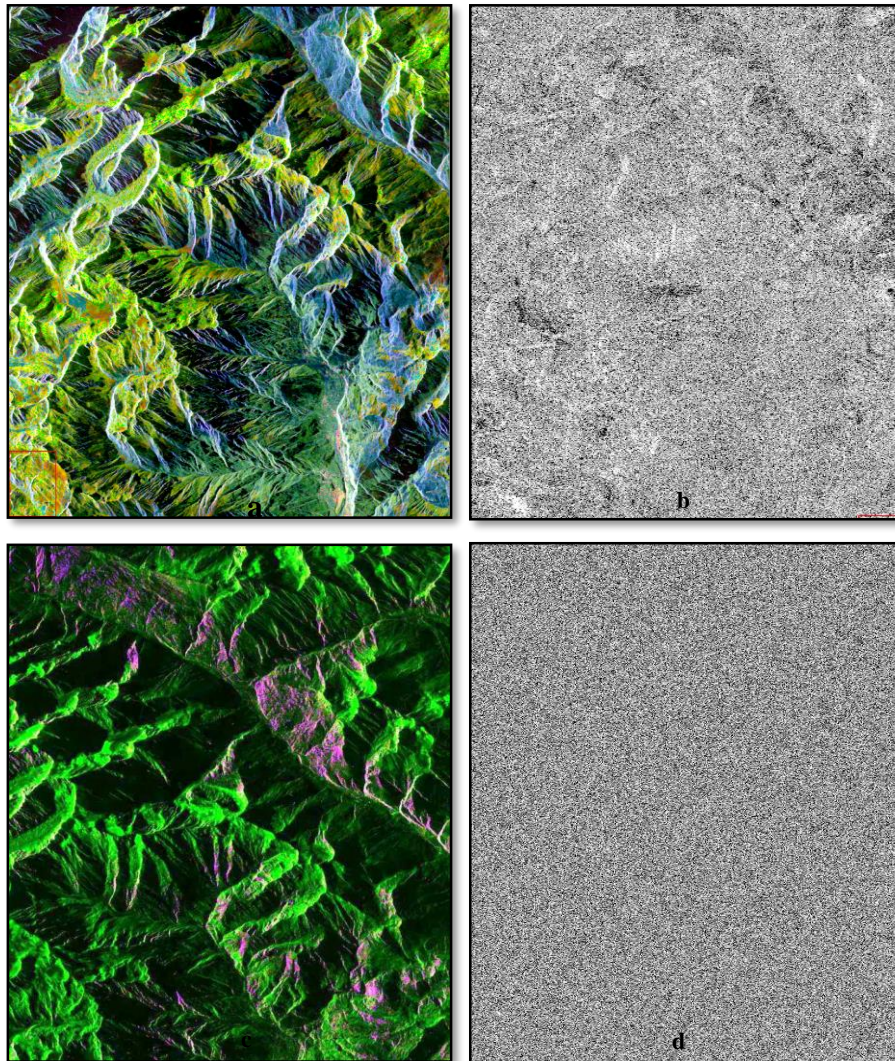


Figure 3- a)- Radarsat-2 Yamaguchi Decomposed RGB Image, b)- Relative Phase Image for Radarsat-2 c)- RISAT-1 yamaguchi decomposed Image, d)- Relative Phase Image for RISAT-1

The fig-3 shows the Co-polar phase coherency and Yamaguchi decomposition for both Radarsat-2 and RISAT-1 FRS-2 datasets. The pattern in co-polar phase coherence was found in the Radarsat-2 dataset (fig-3-b) but it was missing in the RISAT-1 dataset (fig-3-d). The yamaguchi decomposition for the Radarsat-2 and RISAT-1 dataset is shown in fig-3-a and fig-3-c respectively. The over-estimation of the volume scattering (random scattering) was seen in the RISAT-1 datasets. This random scattering was because of the phase incoherency between the co-polar channels, hence the RISAT-1 quad-pol datasets lacks in co-polar phase coherence which makes it unsuitable for yamaguchi decomposition and stokes' based analysis.

4.2 Checking relative phase Image(HH-VV) for Snow

The relative phase was calculated for both the datasets Radarsat-2 and RISAT-1 in the previous section 4.1. Here the analysis of the relative phase image for the snow cover is shown. RISAT-1 quad pol data was found random and it don't relate the target scattering properties (fig-5). The relative phase image using radarsat-2 data shows the phase histogram of the scattering from the snow and variation in the relative phase is seen across the different targets.

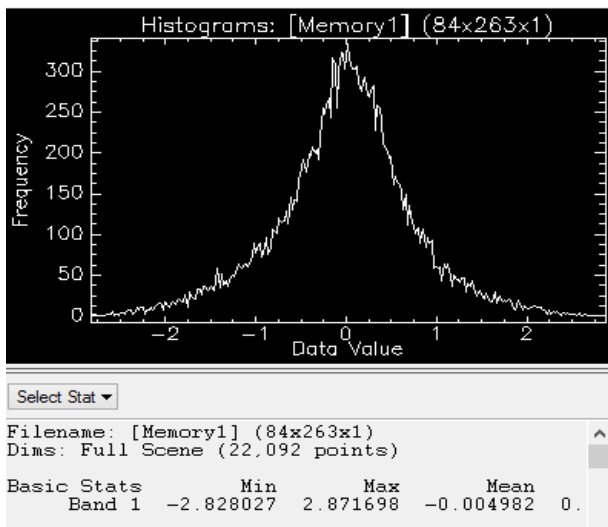


Figure 4-Radarsat-2 relative phase curve for snow

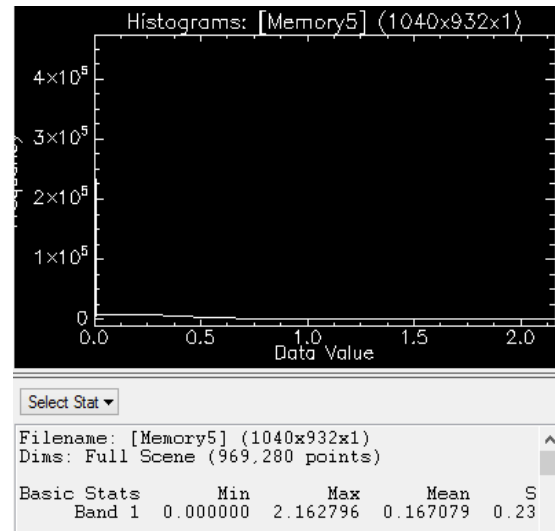
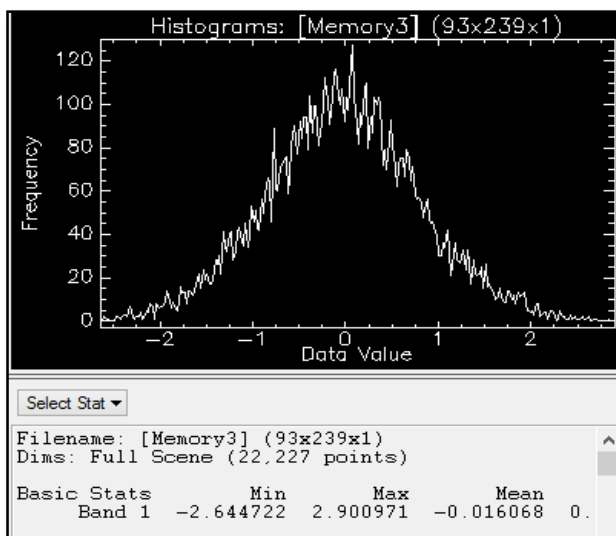


Figure 5-RISAT-1 relative phase Image curve for snow

4.3 Checking relative phase Image(HH-VV) for Vegetation

The diffused random scattering from the vegetation is received by the sensor. For the vegetation the relative phase was calculated for both the datasets. Again RISAT -1 quad pol dataset was not able to relate the relative phase with the target scattering property. In the Radarsat-2 fully polarimetric dataset, volume scattering was related with the relative phase and the generated phase histogram shown in fig-6..



4 Figure 6-Radarsat-2 relative phase curve for vegetation

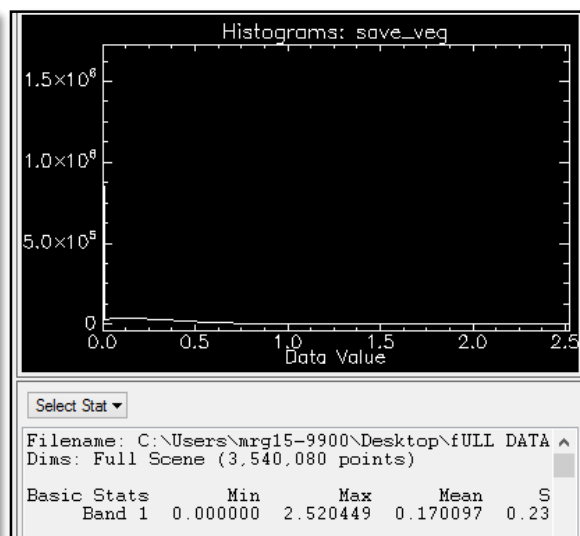


Figure 7-RISAT-1 relative phase Image curve for vegetation

For a monostatic Synthetic Aperture Radar like RISAT-1 it is expected that the both the cross polar channels will produce the similar intensities, resulting in the similar backscattering values in the VH and HV polarization irrespective of the target types. We consider HV= VH for a fully polarimetric data. The Cross-channel HV and VH polarizations has been shown in fig-8 and fig-9 respectively. The variation in the power distribution is shown for both the polarization channels.

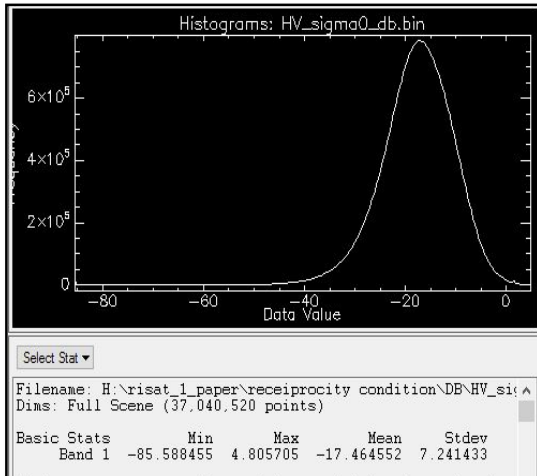


Figure 8-Histogram plot for power in Db for HV RISAT-1 quad-pol datasets

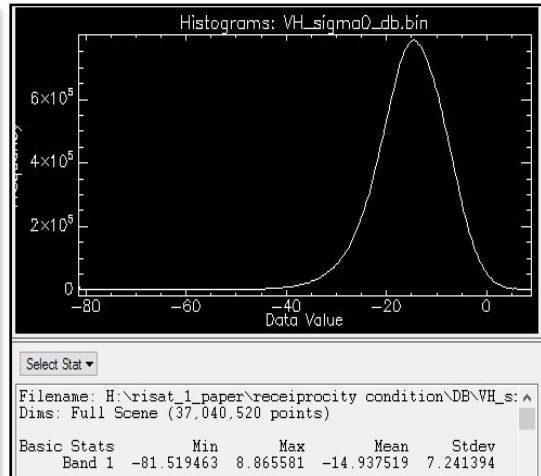


Figure 9-Histogram plot for power in dB for VH polarizations in RISAT-1 quad-pol datasets

4.3 Degree of Polarization

The Figure 10 and Figure 11 shows the value mean, standard deviation and maximum value for degree of polarization for RISAT FRS-2 and RADARSAT-2 data respectively through bar-graph. Required condition for a data to be Fully Polarimetric data is that value of degree of polarization should come 1 but the mean value of degree of polarization is coming as 0.62 which is not appropriate for a Fully Polarimetric data.

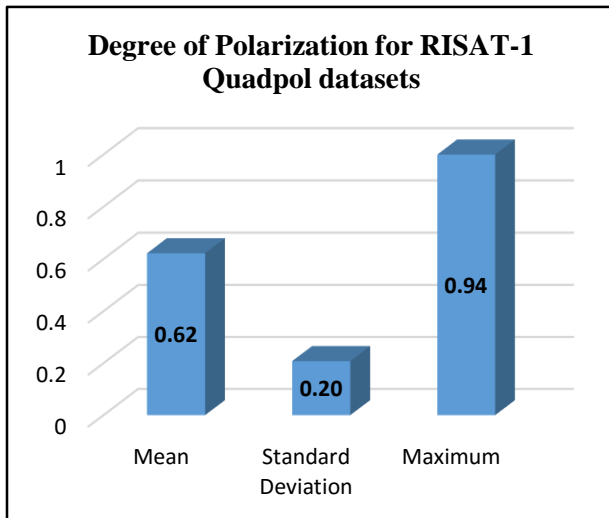


Figure 10-Graphical Visualization of Degree of Polarization for RISAT-1 quad-pol datasets

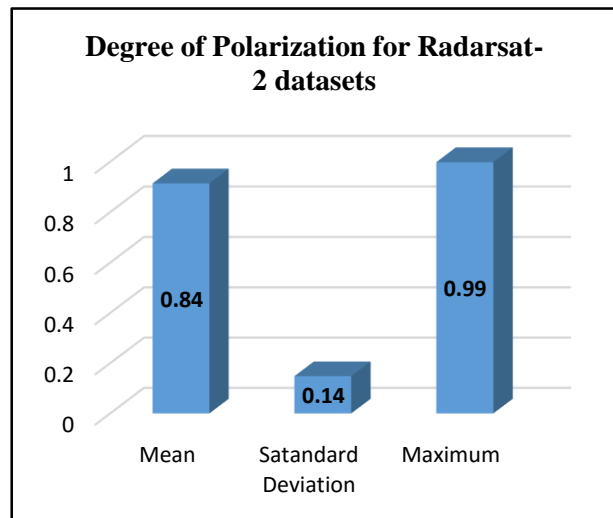


Figure 11-Graphical Visualization of Degree of Polarization for RADARSAT-2 datasets

5 CONCLUSION

RISAT-1 FRS-2 data analysis was done and comparing it with fully polarimetric Radarsat-2 datasets and it was found that RISAT-1 FRS-2 data doesn't have phase coherency across the co-polar channels and hence it can be concluded that this data is not suitable to use it for the stokes' vector based analysis and polarimetric decomposition based analysis.

6 ACKNOWLEDGEMENT

Authors of this paper would like to acknowledge Dr. A.S. Senthil Kumar, Director IIRS and Head Photogrammetry and Remote sensing department IIRS, Mrs. Shefali Agrawal for providing me the opportunity and facilities to do this research work.

7 REFERENCES

- Lee, & Pottier, E. (2009). *Polarimetric radar imaging : from basics to applications*. CRC Press.
- Leinss, S., Parrella, G., & Hajnsek, I. (2014). Snow height determination by polarimetric phase differences in X-Band SAR Data. *IEEE Journal of Selected Topics in Applied Earth Observations and Remote Sensing*, 7(9), 3794–3810. <https://doi.org/10.1109/JSTARS.2014.2323199>
- Mishra, M. D., & Patel, P. (2015). Approach for absolute radiometric calibration of RISAT - 1 SAR data using standard target. *International Journal of Remote Sensing & Geoscience*, 4(1).
- Rao, Y. S., Meadows, P., & Kumar, V. (2016). Evaluation of RISAT-1 compact polarization data for calibration. In *2016 IEEE International Geoscience and Remote Sensing Symposium (IGARSS)* (pp. 3250–3253). IEEE. <https://doi.org/10.1109/IGARSS.2016.7729841>
- Rodionova, N. V. (2009). Phase difference application in fully polsar images. *European Space Agency, (Special Publication) ESA SP, 668 SP*(April), 26–30.
- Yamaguchi, Y., Yajima, Y., & Yamada, H. (2006). A four-component decomposition of POLSAR images based on the coherency matrix. *IEEE Geoscience and Remote Sensing Letters*, 3(3), 292–296. <https://doi.org/10.1109/LGRS.2006.869986>
- Yamaguchi, Moriyama, T., Ishido, M., & Yamada, H. (2005). Four-component scattering model for polarimetric SAR image decomposition. *IEEE Transactions on Geoscience and Remote Sensing*, 43(8), 1699–1706. <https://doi.org/10.1109/TGRS.2005.852084>